

**THE COMPLEX CORE OF ABELL 2199:
THE X-RAY and RADIO INTERACTION**

F. N OWEN

National Radio Astronomy Observatory¹
P.O. Box O, Socorro NM 87801, USA

J. A. EILEK

Physics Department and Astrophysics Research Center
New Mexico Tech, Socorro NM 87801, USA

¹The National Radio Astronomy Observatory is operated by Associated Universities, Inc., under contract with the National Science Foundation.

Received _____; accepted _____

ABSTRACT

The cluster Abell 2199 is one of the prototypical “cooling flow” clusters. Its central cD galaxy is host to a steep-spectrum radio source, of the type associated with cooling cores. In this paper we combine radio data with new ROSAT HRI data to show that conditions in its inner core, $\lesssim 50$ kpc, are complex and interesting. Energy and momentum flux from the radio jet have been significant in the dynamics of the gas in the core. In addition, the Faraday data detects a dynamically important magnetic field there. The core of the X-ray luminous gas is not a simple, spherically symmetric cooling inflow. In addition, we believe the X-ray gas has had strong effects on the radio source. It seems to have disrupted the jet flow, which has led to dynamical history very different from the usual radio galaxy. This particular source is much younger than the galaxy, which suggests the disruptive effects lead to an on-off duty cycle for such sources.

Subject headings: galaxies:clusters:individual(Abell 2199)—
galaxies:individual (NGC6166,3C338)—galaxies:elliptical and
lenticular, cD—galaxies:jets— galaxies:magnetic fields—radio
continuum:galaxies—X-rays:galaxies

1. Introduction

Cluster cores are interesting places. Many cluster centers have steep X-ray profiles and low X-ray temperatures, which have led to models of spherically symmetric cooling flows (*e.g.* the review of Fabian 1994). It is becoming clear however that the central regions are more complex than this simple picture. There is evidence for transonic, turbulent flows (*e.g.* Baum 1992) and for dynamically important magnetic fields (Taylor, Barton & Ge 1994; Eilek, Owen & Wang 1997), at least in the inner $\sim 10 - 50$ kpc of strongly cooling cluster cores.

In addition, when the central galaxies in cooling cores host radio galaxies, these radio sources are not typical. They are more diffuse in appearance and have steeper radio spectra than most larger-scale radio sources (*e.g.*, Burns 1990; the halo of M87 is also a nearby example of this class, *e.g.*, Feigelsen *et al.* 1987). It seems very likely that these sources have a different dynamical history than the larger-scale ones not generally found in cluster centers, and that their history has been affected by their position in the center of a dense cooling core.

In this paper we combine X-ray and radio data to study the central dynamics of one such cooling-core cluster, Abell 2199, with its embedded radio galaxy, 3C338. This cluster seems quite normal dynamically, with no strong evidence of subclumps in velocity data (Zabludoff *et al.* 1990). It contains a central cD galaxy, NGC 6166. This galaxy appears to have a triple nucleus, which is likely to arise from a projection of very eccentric orbits (Lauer 1986) rather than from a tightly bound central system. The cluster redshift is $z = .0312$ (Hoessel, Gunn & Thuan 1980), so that 1 arcmin corresponds to 36 kpc if $H_o = 75$ km/s-Mpc.

The X-ray distribution from this cluster is also quite regular, indeed rather dull, on large scales. The Einstein image (Forman & Jones 1982) shows smooth, roughly circular

isophotes. Jones & Forman (1984) quote a core radius ~ 210 kpc (converted to our $H_o = 75$ km/s-Mpc). The smooth distribution shows no particular signs of subclumping or merger activity. This cluster is one of the prototypical cooling cores: the inner regions show the characteristic X-ray excess relative to a King-model fit. Arnaud (1985) finds a cooling radius ~ 120 kpc, a central cooling time ~ 0.8 Gyr, and a mass inflow $\sim 90M_{\odot}/\text{yr}$. The more detailed cooling-flow model of Thomas, Fabian & Nulsen (1987) has similar numbers.

NGC 6166 contains a radio source, 3C338. It is small (radial extent ~ 35 kpc) moderate power (8.8×10^{41} erg/s between 10 MHz and 100 GHz, data from Herbig & Readhead 1992, converted to $H_o = 75$ km/s-Mpc), steep spectrum (the integrated spectrum is given in Herbig & Readhead, and two-frequency spectral index distribution in Burns, Schwendeman & White 1983), and diffuse in appearance. Thus it fits well in the class of cooling-core radio sources. Newer radio data have been obtained by Feretti *et al.* (1993), who present VLB images of a two-sided core jet, and by Ge & Owen (1994), who made new VLA images with polarization and Faraday rotation data.

In this paper, we combine new ROSAT data with existing radio data to explore the interesting dynamics of the core of A2199. We find direct evidence of the effect of the radio source on the central X-ray luminous gas. In this region, at least, we find that the X-ray gas cannot be described by a simple, spherical cooling flow model. We then compare this radio source with standard models for “normal” radio sources, and conclude that this source is relatively young and has been disrupted by the surrounding gas. We suspect that this scenario may be typical of the class of cluster-center radio sources.

2. The Data: The Central Regions of A2199

The intracluster medium (ICM) in Abell 2199 is smoothly distributed on large scales, and appears to be sitting quietly in the potential well of the central galaxy. In Figure 1 we show an optical image of the central ~ 4 amin of the cluster (the data were taken by Owen & White 1991). The elongation of the low surface brightness halo of NGC 6166 is apparent. Lauer (1986) finds the position angle of the optical isophotes $\sim 30^\circ$, for the inner ~ 30 asec; Owen & White find the same position angle for the 24.5 mag/asec² isophote, on a scale of ~ 100 asec ~ 60 kpc. As we shall show, the large-scale X-rays are consistent with this.

We obtained ROSAT HRI data of the inner ~ 1000 asec (~ 600 kpc) of the cluster. A total of 47,522 seconds of useful integration time was accumulated by the satellite in 1994 on Abell 2199. The observations were made during two time periods, 3Feb94 to 5Feb94 and 31Aug94 to 6Sep94, each with about half the total integration time. The 17 amin area we studied has 166,725 detected photons. Using 2 arcsec pixels the peak on the image (at the nucleus of NGC6166) had 27 photons. No identifications of discrete sources with optical objects were found on the combined image except for the core of the central galaxy. Thus no checks were possible on the default coordinate system. However, the positional agreement between the two parts of the integration are good, agreeing within about 2 arcsec in each coordinate for the brighter discrete sources in the field, so we have adopted the default coordinate system. The photon statistics are not good enough to attempt to track any pointing wander as in Morse (1994). However, the discrete sources within 6 amin of the nucleus in the final image are consistent with FWHM of about 6 asec EW and slightly less NS. Since the peak on the image is not very large, features much larger than this are probably real. At the resolution we have have used to display the x-ray emission, all the features described are seen on images made with either dataset.

In Figure 2 we show a contour map of the field, smoothed to 56 asec resolution. We

note that the isophotes remain smooth, with no particular evidence of substructure, and show a only modest ellipticity. We binned the unsmoothed data into circular rings to derive a luminosity profile, which is shown in Figure 3. The error bars in this figure assume Gaussian noise. From ~ 1 amin to ~ 10 amin, the surface brightness follows a power law, $S_x(R) \propto R^{-1.2}$ if R is the projected distance from the center. At smaller projected radii, our surface brightness profile continues to rise inwards, but less rapidly. The Einstein data of Jones & Forman (1984) show a steeper falloff on larger scales, $S_x(R) \sim R^{-2.2}$ for $R \gtrsim 5$ amin. Thus, a single power law is not a good fit to the entire cluster. We inverted the surface brightness with an Abel transform to find the radial emissivity profile of the cluster, out to ~ 10 amin.¹ To get the gas density, we assumed a temperature $T = 2 \times 10^7$ K (consistent with Thomas, Fabian & Nulsen 1987) throughout the cluster. (We note that the emissivity in the ROSAT band is not a sensitive function of the temperature, in this temperature range; this should provide a reliable measurement of the density). We estimated the error in the deprojection by adding noise to each data point, chosen randomly in a $\pm\sigma$ range around the data; we repeated this random choice, and the Abel inversion, 100 times and determined the mean and standard deviation of the result. Our final density profile is shown in Figure 4. The gas density derived from this analysis also follows a good power law, $n_X(r) \propto n^{-1.2}$ past $r \sim 60$ kpc. Inside of this it rises more gradually, as $n_X(r) \propto n^{-2/3}$, and approaches $n \sim 0.06 \text{ cm}^{-3}$ as $r \rightarrow 0$.

In Figure 5 we show the ellipticities, and position angles, of elliptical isophotes fitted to the X-ray image using the IRAF program ELLIPSE. This program works it way from

¹In order to reduce edge effects in the transform, we artificially extrapolated the measured $S_X(r)$, following the observed power law well past the last measured data point. This technique reduces the artificial turnup at large r brought about by edge effects, but of course adds an unsupported assumption to the large-scale structure we derive for scales $\gtrsim 200$ asec.

the solution at one radius to the next by considering a radius larger (or smaller) by a given fraction. In this case the fraction used was 0.1. For this reason the inner part of the profile is oversampled and the errors are not independent. This does not affect any of the later analysis. On scales $\gtrsim 80$ asec (~ 50 kpc) the ellipticities and position angles remain approximately steady, at $\epsilon \sim 0.2$ and $\theta \sim 35^\circ$, respectively. We note that the isophotes are not very elliptical, so that our spherically symmetric Abel inversion should be valid. In addition, in Figure 6 we show an overlay of optical contours on the X-ray image, which demonstrates that the position angle of the large-scale X-ray isophotes correlates well with the structure of the central galaxy.

Thus, the outer regions of the X-ray gas seem to be sitting quietly in the potential well of the galaxy. The region inside $\sim 50 - 60$ kpc is more interesting, however. This is the region inside of which the X-ray isophotes (Figure 5) change position angle and shape. For $r \lesssim 20$ asec the isophotes have $\theta \sim 80^\circ$; at this point they rotate abruptly to $\theta \sim 15^\circ$; past here they gradually rotate into alignment with the outer values. The ellipticity also changes; the very inner isophotes have $\epsilon \sim 0.2 - 0.3$; at $r \sim 20$ asec they become round ($\epsilon \sim 0$); past this they flatten slightly to agree, again, with the outer values.

In addition, the volume within ~ 50 asec is that occupied by the radio source. In Figure 7 we show the 5 GHz image of 3C338 from Ge & Owen (1994). The radio core coincides with the nucleus of NGC 6166 (Ge & Owen 1994), and also with the peak of the X-ray image using the coordinate system provided with the ROSAT database. A short jet, apparently ending in hot spots, is visible on either side of the core, extending ~ 3 kpc to a pair of hot spots. A two-sided nuclear jet has been detected on VLB scales (Feretti *et al.* 1993). The orientation of this jet coincides with the inner jet and hot spots on the VLA image. The bright ridge, or filament, south of the radio core does not coincide with any stellar feature; it is likely to be simply a high-emissivity filament, as is common in other

sources (*e.g.* M87, Hines, Owen & Eilek 1989; 3C442, Comins & Owen 1991). The more diffuse radio lobes extend to ~ 35 kpc from its core, in our image and also in that of Burns *et al.* (1983). Roland, Hanisch & Peltier (1990) searched but found no evidence for more extended, diffuse emission; the source seems to stop at ~ 35 kpc. We point out that the diffuse lobes also show non-uniform, filamentary internal structure.

The radio data also shows that the inner core contains magnetized thermal plasma (in addition to the magnetized relativistic plasma within the radio source). The Faraday rotation data of Ge & Owen (1994) show that rotation measures ~ 1000 rad/m², ordered on scales ~ 3 kpc, exist in the inner core. In the next section we show that this is evidence of a dynamically important magnetic field in the core.

The complex dynamics of the inner core is also apparent in the central parts of the X-ray image. In Figures 8 and 9 we show X-ray emission from the inner core, at higher resolution (7.5 arcsec), with the radio contours overlaid. From both figures it is apparent that the radio source and X-ray luminous gas know about each other. Figure 8 shows that the inner X-ray gas extends almost directly to the north, for ~ 40 arcsec, at a right angle to the radio jet direction. Figure 9 shows that the very innermost X-ray gas is elongated east-west about 20 arcsec, showing “ears” that coincide with the two radio hot spots at the ends of the inner jet.

Thus, the images suggest that the X-ray and radio sources are interacting on scales $\lesssim 50$ kpc in the inner core. In the next section we explore this interaction.

3. Discussion: Dynamics of the Centre

The data show that the central regions of A2199 are not simple. The radio source and the X-ray luminous gas are interacting strongly. Existing “standard” models for each

component (cooling flows for the X-ray gas, jet-driven dynamics for the radio source) must be modified to account for this interaction.

3.1. The Central Regions of the Cluster Plasma

The dynamics of the central ~ 50 kpc of A2199 are not well described by a spherically symmetric, cooling-flow model. We find that the core contains a dynamically significant magnetic field, and that the radio source has a strong effect on the dynamics of the gas core.

The polarization data of Ge & Owen (1994) show that the core has a significant, ordered RM distribution, and that the RM must come from foreground gas. In particular, the RM does not appear consistent with a totally random magnetic field; as with other sources (*e.g.*, Taylor *et al.* 1994, or Eilek *et al.* 1997), the sign and magnitude of the RM has a consistent, ordered pattern. We identify the foreground gas as the X-ray luminous gas in the cluster core. Taylor & Perley (1993) and Ge & Owen (1993) showed that the rotation-producing gas in Hydra A and Abell 1775, respectively, is neither within the radio source, nor from embedded emission-line clouds, nor in a mixing layer between the radio source and the cluster gas. Their arguments also apply to Abell 2199; thus we take the X-ray bright cluster gas to be the source of the rotation.

The data show that the RM has a typical magnitude ~ 750 rad/m²; it has a typical order scale ~ 3 kpc. The depth of the RM patch along the line of sight is likely to be comparable, also ~ 3 kpc; as the source is larger than this, we are likely seeing “patches” or “flux ropes” of this scale, in front of the source. If this typical RM comes from gas at density 0.02 cm⁻³ (which we take as a typical value for the region from ~ 4 to ~ 80 asec), the mean line-of-sight magnetic field is $\langle B_{\parallel} \rangle \sim 15\mu\text{G}$. If we increase this by a $\sqrt{3}$ factor to account for likely projection, we estimate the mean magnetic pressure in the lobe region

$\sim 2.8 \times 10^{-11}$ dyn/cm². For comparison, the pressure of the X-ray luminous gas in this region is $p_g = nkT \simeq 5.6 \times 10^{-11}$ dyn/cm² (for typical values in this core, we estimate $n \sim 0.02$ cm⁻³ from our deprojection, and $T \sim 2 \times 10^7$ K as above). The typical magnetic pressure is thus significant compared to the ambient gas pressure.

The RM data also show one smaller, high-RM patch: a region with $RM \sim 1200$ rad/m², with scale ~ 300 pc, to the west of the nucleus (which can be seen in Figure 3 of Ge & Owen 1994). If this is also the line-of-sight scale, this filament has $\langle B_{\parallel} \rangle \sim 250 \mu\text{G}$, and a minimum $p_B \sim 2.5 \times 10^{-9}$ dyn/cm². This is significantly higher than the ambient X-ray gas pressure. This suggests that the feature is strongly overpressured, and either locally self-confined magnetically, or else transient. It is also possible, of course, that the RM of this filament is increased by local density fluctuations or a chance projection (with a longer line of sight, if we are looking along a long filament), or that the feature is somehow locally confined by its own field. Again, this says that the core plasma is magnetized, at a level which is important to its dynamics.

We also find that the gas distribution of the inner core has been affected by the radio source. As we pointed out above, inside of ~ 50 kpc the distribution of the X-ray gas changes from the uniform ellipticity and position angle it shows on larger scales. In particular, the axes of the radio jets and of the inner X-ray isophotes are clearly connected (as in Figures 8 and 9). These images suggest the following picture.

On the smallest scales, the radio jet is transferring momentum to the X-ray gas, pushing it out and causing the “ears” of X-ray emission around the jet. For instance, Chernin *et al.* (1994) modelled supersonic jets moving through a medium with a short cooling time. They find that high Mach number jets can transfer significant momentum to the ambient gas, *at the head of the jet*. Their calculation may be relevant here. Picking $n = 0.05$ cm⁻³ for the inner few kpc, $T = 2 \times 10^7$ K and using the Raymond *et al.* (1976)

emissivities gives a cooling time ~ 130 Myr. This is only a few times larger than the dynamical age of the source, which we argue in the next section is on the order of tens of Myr.

In addition, The X-ray isophotes are elongated to the immediate north of the jet, opposite to the direction of the radio lobes. This suggests that power from the radio source has been deposited in the inner X-ray gas, causing this structure. Quantitative estimates of the energetics of the core seem consistent with this. Recall $P_{rad} \sim 8.8 \times 10^{41}$ erg/s. The beam power is most likely much larger (*e.g.*, Eilek & Shore 1989). If we guess $\sim 1\%$ as a typical efficiency, the beam power is $P_b \sim 10^{44}$ erg/s. Much of this beam power will be deposited in the ambient gas, as well as in the radio lobes themselves. We first note that the bolometric luminosity from the X-ray gas, using the Raymond, Cox & Smith (1976) emissivities, is $L_{core} \sim 2.4 \times 10^{43}$ erg/s. (We calculated this for the inner 35 kpc of the X-ray core, the size of the radio lobes.) This is very similar to the likely P_b value. Thus the beam power clearly has a strong effect on the local thermal balance of the X-ray gas.

We can also estimate the energy content of the inner 35 kpc of gas. Its thermal energy content is $U_x = \frac{3}{2}p_x \simeq 2.6 \times 10^{59}$ erg; its gravitational potential energy will be similar. The radio beam deposits this much energy in a time $U_x/P_b \simeq 81/P_{44}$ Myr. This again argues that the radio source has had a significant effect on the energetics of the inner core, and can have heated the “northern extension” of the X-ray gas enough to move it upwards in the local gravitational potential.

3.2. The Cluster-Center Radio Source

The radio source 3C338 is typical of steep-spectrum cluster-center radio sources. We suggest that it has developed from a jet which has been severely disrupted, by the conditions

in the central cooling core of this cluster. It follows that this is a relatively young source; and that such cluster-center galaxies must have an “on/off” cycle of radio activity.

We begin our argument with the appearance of the source. It is more diffuse than standard Type I or Type II radio galaxies; it shows neither strong external hot spots nor a directed tail flow emanating from the core. It does contain an active VLB jet, which connects to the 3-kpc scale VLA inner jets but does not continue into the lobes. Its diffuse appearance suggests that it has grown more as a “bubble”, driven by its internal energy, than as a standard source driven by directed jet flow. The lobes are not particularly uniform. They are inhomogeneous, breaking up into filaments as in Figure 7; there is one bright ridge to the south of the core; and they are located to one side of the central core (opposite to the X-ray extension).

We also point out that the radio plasma must be separate from the X-ray luminous gas. If the two plasmas were well mixed, the high rotation measure found by Ge & Owen (1994) would depolarize the source (for example, a rotation measure of 750 rad/m² gives a Faraday depth ~ 1.8 radians at 6 cm; this would easily depolarize the source). Thus the radio plasma cannot be well-mixed with the local X-ray gas. This argues against diffusion as the origin of this source, and supports our suggestion of a ‘separate ‘bubble’.

The pressure within the radio source is consistent with our picture. We calculated the minimum pressure for the bright filament to the south of the radio core, and also for the diffuse lobes. In doing the calculation, we took the high-frequency spectral index $\alpha = 1.7$ from Burns *et al.* (1983), but assumed the spectrum flattened to $\alpha = 1.0$ between 10^7 Hz and 10^9 Hz. (This give a more conservative estimate for the minimum pressure.) We also assumed a uniformly filled source, and equal energy densities in relativistic protons and electrons. We found $p_{min} \simeq 1.2 \times 10^{-10}$ dyn/cm² for the bright filament (corresponding to $B_{min\ p} \simeq 42\mu\text{G}$), and $p_{min} \simeq 4.8 \times 10^{-12}$ dyn/cm² for the diffuse regions (giving

$B_{min\ p} \simeq 8\mu\text{G}$). Thus, the bright filament is overpressure relative to the X-ray background (recall $p_x \sim 5.6 \times 10^{-11}$ dyn/cm² is typical of the inner ~ 40 kpc), while the lobes have $p_{min} < p_x$. The latter condition is compatible with pressure balance, because the true pressure in the radio source can exceed p_{min} easily; this will occur either if the source is inhomogeneous (as it clearly is), or if it is not exactly at the minimum pressure condition (which is physically quite possible). We suspect that overall pressure balance is maintained, and that the bright filament to the south is a transient feature, currently overpressured, for instance due to strong turbulence in the region.

What, then, is the dynamical history of this source? We suspect that the nuclear jet became unstable and disrupted severely, at approximately its current position of ~ 3 kpc from the core. We are not aware of numerical simulations which specifically address this situation. Hardee *et al.* (1992) modelled jets propagating in atmospheric gradients. Loken *et al.* (1994) modelled jets propagating in a strong cooling inflow. Both found that jets with lower Mach number can be stalled out or suffer strong instabilities which dramatically slow their propagation. After the instability has developed, the material flowing through the jet fills a “lobe” or “bubble” which grows only slowly thereafter. This bubble has now reached the lobe size, ~ 35 kpc. While neither of these calculations addresses the conditions which we find in A2199 – a magnetized, probably turbulent, ambient medium – we suspect similar evolution may occur in this case.

If we adopt this model we can estimate the dynamical age of the radio source. One clue comes from the 3 kpc length of the jet. Following Scheuer (1974), we apply momentum flux balance at the end of the jet. This predicts that a jet of opening angle Ω , beam power P_b and speed v_b propagates into an ambient medium of density ρ_x at a rate given by

$$D(t) \simeq \sqrt{2} \left(\frac{P_b}{\Omega v_b \rho_x} \right)^{1/2} \quad (1)$$

where Ωv_b relates the beam power to its momentum flux. Models of Type II RS (Eilek

1997a) suggest $\xi = 100\Omega v_b/c \sim 1$, and we use this scaling here as well. Taking $n_x \simeq 0.02$ from our X-ray data, the jet length expression becomes

$$D(t) \simeq 0.84 \left(\frac{P_{44}}{\xi} \right)^{1/4} t_{Myr}^{1/2} \text{ kpc} \quad (2)$$

for propagation into a uniform medium at the density of the central X-ray gas. This predicts that the jet reaches 3 kpc in $t_{jet} \sim 17$ Myr if $P_{44}/\xi = 1$. We suspect that it reached this point in this time, then suffered strong instabilities and disruption; thereafter mass and energy transport continued, but not as a collimated flow. The source must therefore be at least as old as this.

A second constraint on the age comes from the expansion of the lobes. We envision them growing due to the internal pressure of the plasma which has passed through the end of the (now stalled) jet. Following Eilek & Shore (1989), we describe the evolution of such a lobe which expands at approximate pressure balance with its surroundings:

$$V(t) \simeq \frac{P_b}{p_x} t \quad (3)$$

Taking the X-ray pressure, $p_x \simeq 5.6 \times 10^{-11}$ dyn/cm², with $V = 4\pi R^3/3$ (ignoring non-sphericity), gives an estimate of the linear scale of the lobe:

$$R(t) \simeq 7.8 (P_{44} t_{Myr})^{1/3} \text{ kpc} \quad (4)$$

so that the lobes have reached their current 35 kpc size in $t_{vol} \sim 90$ Myr if $P \simeq 10^{44}$ erg/s. Our picture is self-consistent, in that this time is longer than the time needed for the central jet to reach its current scale.

One caveat here is that these calculations assume propagation into a uniform external medium. In reality the ambient X-ray gas has a strong density and pressure gradient, as is apparent from Figures 3 and 4. This will accelerate both the jet propagation and the lobe growth. We are not aware of any specific models of such propagation, but expect such

affects to, say, reduce t_{jet} and t_{vol} by a factor of 2 or so. In addition one might expect bouyancy to be important in the lobe growth. This is also not included; we can estimate its effect by arguing that bouyant velocities will be no larger than the local gravitational speed. Fisher, Illingworth & Franx (1995) measure the velocity dispersion $\sigma \sim 270$ km/s for NGC 6166; from this we can estimate $t_{bouy} \sim 35 \text{ kpc} / \sqrt{3}\sigma \sim 60$ Myr. This is comparable to t_{vol} , suggesting that bouyancy will also reduce the growth time by an order-unity factor.

Another possible estimate of the source age is from spectral steepening. Burns *et al.* (1983) take 400 MHz as the turnover frequency. If this applies throughout the source, we derive synchrotron ages of ~ 70 Myr for the diffuse lobes (with $B_{min\ p} \sim 8\mu\text{G}$), and ~ 6 Myr for the bright filament (with $B_{min\ p} \sim 42\mu\text{G}$). The larger of these numbers appears consistent with our dynamical ages. We caution, however, that spectral steepening by itself is not a reliable estimate of source ages; Eilek (1997b) demonstrates this for Type I sources, and Eilek, Melrose & Walker (1997) discuss an alternative interpretation of the spectrum. Thus, we regard the coincidence of this estimate with our dynamical ages as interesting, but not definitive.

Thus, our dynamical picture suggests that the source is young; it has taken no more than several tens of Myr to reach its current size. This is significantly younger than the age of the parent system.

4. Conclusions

In this paper we presented new X-ray data which shows evidence of a complex interaction between the two plasmas (relativistic, radio bright, and thermal, X-ray bright) in the core of A2199. We draw two major conclusions from this.

First, the core of this prototypical “cooling flow” is a complex place. The magnetic

energy density (and one suspects turbulent energy densities) are comparable to that of the thermal gas. The radio source is an important source of energy to the X-ray gas in the core. Thus, this is not a simple symmetric cooling flow, at least on these scales. Second, the radio source shows signs of being disrupted by the ambient gas. It remains unmixed with the X-ray gas, but has a different dynamical history than most radio galaxies. We suspect this is a clue to the unusual nature of steep-spectrum, cluster-center radio sources.

It is worth noting that M87 is another very similar example of this phenomenon. The large-scale radio halo of M87 (*e.g.*, Feigelsen *et al.* 1987) has a similar, diffuse appearance, and similar linear scale. The inner radio source of M87 has a jet which clearly disrupts on a scale of a few kpc (*e.g.*, Owen, Hardee & Cornwell 1989). The total radio power of M87 is very close to that of 3C338 (Herbig & Readhead 1992), although the minimum pressure in the diffuse radio lobes is lower for M87 (Feigelsen *et al.* 1987). The inner regions of the X-ray halo of M87 have a similar run of pressure (Nulsen & Böhringer 1995), and also show evidence of dynamical interaction with the radio galaxy (Böhringer *et al.* 1995). Finally, the nuclear gas – at least on the few kpc scale – is also strongly magnetized (Owen, Eilek & Keel 1990). Thus, at least one other system seems very similar to the one we have studied here

Finally, we note that steep spectrum radio sources are common in cD's in cooling cores; Burns (1990) detected such sources in $\sim 2/3$ of his sample. While most have not been studied in detail, we suspect that 3C338 and M87 are typical members of this class. If this is the case, the central cD must be radio-active for most of its life. This can only be reconciled with the relatively young age we deduce for 3C338 ($\sim 30 - 100$ Myr) if the parent galaxy has frequent, short-lived radio-active periods. Perhaps the instabilities which we see now disrupting the jet, eventually shut it off totally, and after a quiescent period the system restarts itself?

We thank Chris Loken for useful discussions on jet disruption, and Fang Zhou for his help with the data. JE was partially supported by NASA grant NAG51848 and NSF grant AST-9117029.

REFERENCES

- Arnaud, 1985, *Ph. D. thesis*, Cambridge University.
- Baum, S., 1992, in Fabian, A. C., ed, Clusters and Superclusters of Galaxies (Dordrecht: Kluwer), 171.
- Bohringer, J., Nulsen, P. E. J., Braun, R. & Fabian, A. C., 1995, MNRAS, 274, L67.
- Burns, J. O., 1990, AJ, 99, 14.
- Burns, J. O., Schwendeman, E. & White, R. A., 1983, ApJ, 271, 575.
- Chernin, L., Masson, C., Dal Pino, E. M. & Benz, W., 1994, ApJ, 426, 204.
- Comins, N. F. & Owen, F. N., 1991, ApJ, 382, 108.
- Eilek, J. A., 1997a, in preparation.
- Eilek, J. A., 1997b, submitted to ApJ.
- Eilek, J. A., Melrose, D. B. & Walker, M. A. W., 1997, ApJin press.
- Eilek, J. A., Owen, F. N & Wang, Q., 1997, in preparation.
- Eilek, J. A. & Shore, S. N., 1989, ApJ, 342, 187.
- Fabian, A. C., 1994, ARA&A, 32, 277.
- Feigelsen, E. D., Wood, P. A. D., Schreier, E. J., Harris, D. E. & Reid, M. H., 1987, ApJ, 312, 101.
- Feretti *et al.*, 1993, ApJ, 408, 446.
- Fisher, Illingworth & Franx, 1995, ApJ, 438, 539.
- Forman, W. & Jones, C. J., 1982, ARA&A, 20, 547.
- Ge J.-P. & Owen, F. N., 1993, AJ, 105, 778.
- Ge J.-P. & Owen, F. N., 1994, AJ, 108, 1523.

- Hardee, P. E., White, R. E. III, Norman, M. L., Cooper, M. A. & Clarke, D. A., 1992, *ApJ*, 387, 460.
- Herbig, G., & Readhead, A., *ApJS*, 81, 83, 1992.
- Hines, D. C., Owen, F. N. & Eilek, J. A., 1989, *ApJ*, 347, 713.
- Hoessel, J. G., Gunn, J. E. & Thuan, T. X., 1980, *ApJ*, 241, 486.
- Jones, C. J. & Forman, W., 1984, *ApJ*, 276, 38.
- Lauer, T., 1986, *ApJ*, 311, 34.
- Loken, C., Burns, J. O., Norman, M. L. & Clarke, D. A., 1993, *ApJ*, 417, 515.
- Morse, J. A., 1994, *PASP*, 106, 675.
- Nulsen, P. E. J., & Böhringer, H., 1995, *MNRAS*, 274, 1093.
- Owen, F. N., Eilek, J. A. & Keel, W., 1990, *ApJ*, 362, 449.
- Owen, F. N., Hardee, P. E. & Cornwell, T. J., 1989, *ApJ*, 340, 698.
- Owen, F. N. & White, R., 1991, *MNRAS*, 249, 164.
- Raymond, J. C., Cox, D. P. & Smith, B. W., 1976, *ApJ*, 204, 290.
- Roland, Hanisch & Peltier, 1990, *Å*, 331, 327.
- Scheuer, P. A. G., 1974, *MNRAS*, 166, 513.
- Taylor, G. B. & Perley, R. A., 1993, *ApJ*, 416, 554.
- Taylor, G. B., Barton, E. J. & Ge, J.-P., 1994, *AJ*, 107, 1942.
- Thomas, P. A., Fabian, A. C. & Nulsen, P. E. H., 1987, *MNRAS*, 228, 973.
- Zabludoff, A. I., Huchra, J. P. & Geller, M. J., 1990, *ApJS*, 74, 1.

Figure Captions

Fig. 1.— Optical image, obtained by Owen & White (1966), of the central region of the cluster Abell 2199. The cD galaxy NGC 6166 dominates the central region of the cluster.

Fig. 2.— The ROSAT HRI image of Abell 2199, smoothed to 56 asec resolution. This choice gives a Gaussian beam of 1 amin^2 . The units in this figure are counts per beam. Note the lack of substructure, and the constancy of the isophote position angles on these scales.

Fig. 3.— The X-ray surface brightness of Abell 2199, obtained by binning the unsmoothed data into circular rings. The units of this figure are counts per pixel, where each image pixel is 2 asec square. Note the shoulder at $r \sim 80 \text{ asec}$, which is approximately the extent of the central radio source 3C 338.

Fig. 4.— The X-ray density of Abell 2199. We derived this using an Abel transform on the data in Figure 3, and assuming a uniform temperature $T \simeq 2 \times 10^7 \text{K}$. Note the shoulder in the density distribution at $\sim 80 \text{ asec}$.

Fig. 5.— (a) The ellipticities of the X-ray isophotes. In this figure and the next, the profile is oversampled close to the nucleus, and therefore the errors in that region are not statistically independent. Note the increasing elongation from $r \sim 0$ to $r \sim 16 \text{ asec}$, the sudden drop there to nearly round isophotes, and the connection past that point to the large-scale $e \sim 0.2$ value. (b) The position angle of the isophotes. Note the dramatic difference between the inner isophotes, whose position angle is at right angles to the jet of the radio source, and the outer isophotes, whose position angles agree with the orientation of the cD galaxy.

Fig. 6.— An overlay of the optical image (contours) and the X-ray image (color), demonstrating the good agreement of the orientation of the stellar galaxy and the X-ray bright gas on these scales.

Fig. 7.— The 20 cm radio image of 3C338, from Ge & Owen 1994. The radio core is in the center of the picture, and is the source of short jets which terminate in the hot spots at ± 3 kpc to either side of the core. The grey-scale display is proportional to the tenth root of the intensity, in order to emphasize the fine structure and diffuse emission more clearly than is shown in Ge & Owen. The core coincides with the galactic nucleus and the VLB core and jet seen by Feretti *et al.*(1993). The bright filament to the south is not a jet; it seems to be simply a high-pressure shock or flux rope in the radio plasma.

Fig. 8.— An overlay of the radio image (contours) and the X-ray image (color). This figure illustrates the $r \lesssim 35$ kpc scales, on which the X-ray gas is elongated north-south and seems to be strongly affected by the radio source.

Fig. 9.— An overlay of the radio and X-ray images, similar to Figure 8, but illustrating the smallest scales ($\lesssim 5$ kpc, seen as the orange-red central region), on which the X-ray gas is elongated east-west, and seems to be receiving momentum transferred from the radio jet.

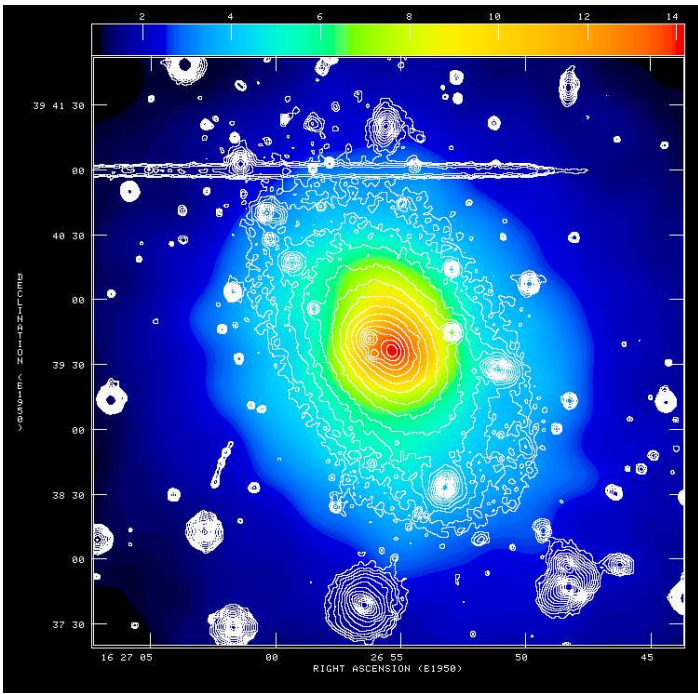


Figure 6: X-ray/Optical Overlay

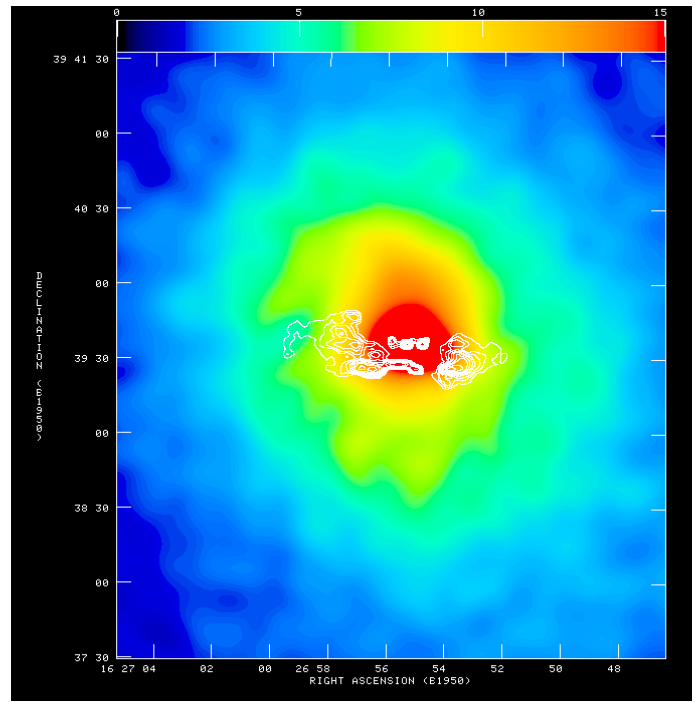


Figure 8: Radio/X-ray Overlay

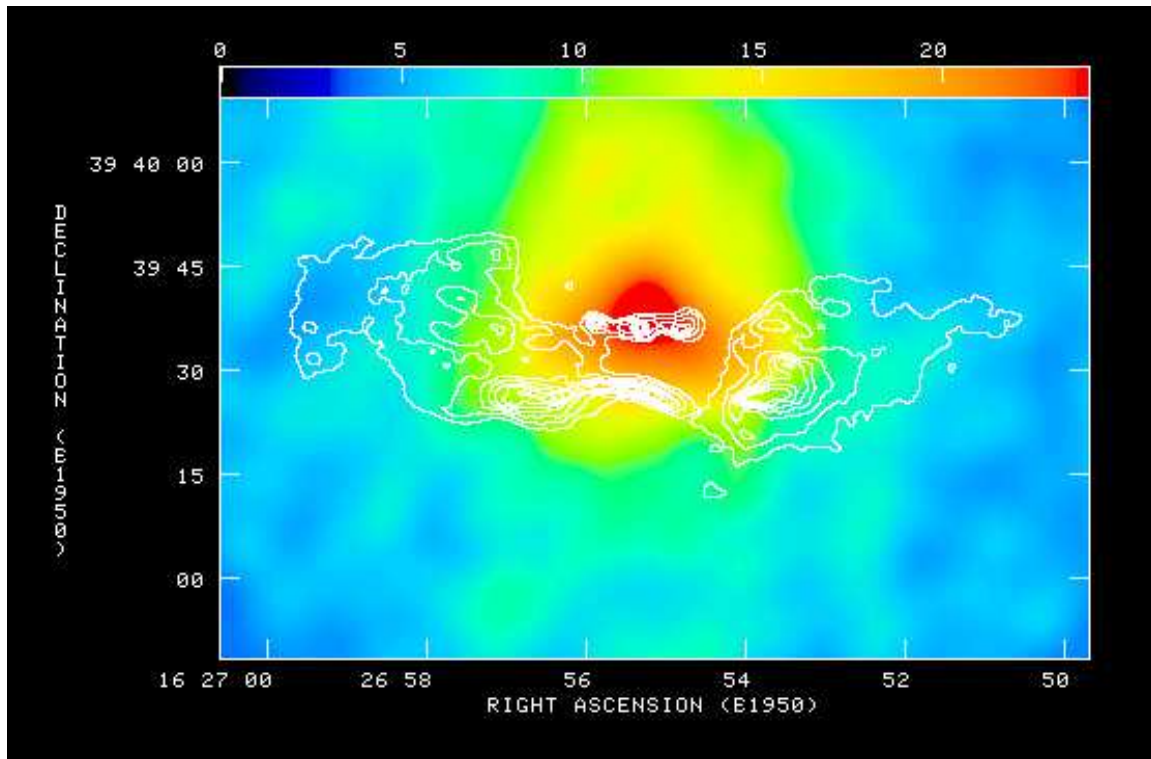
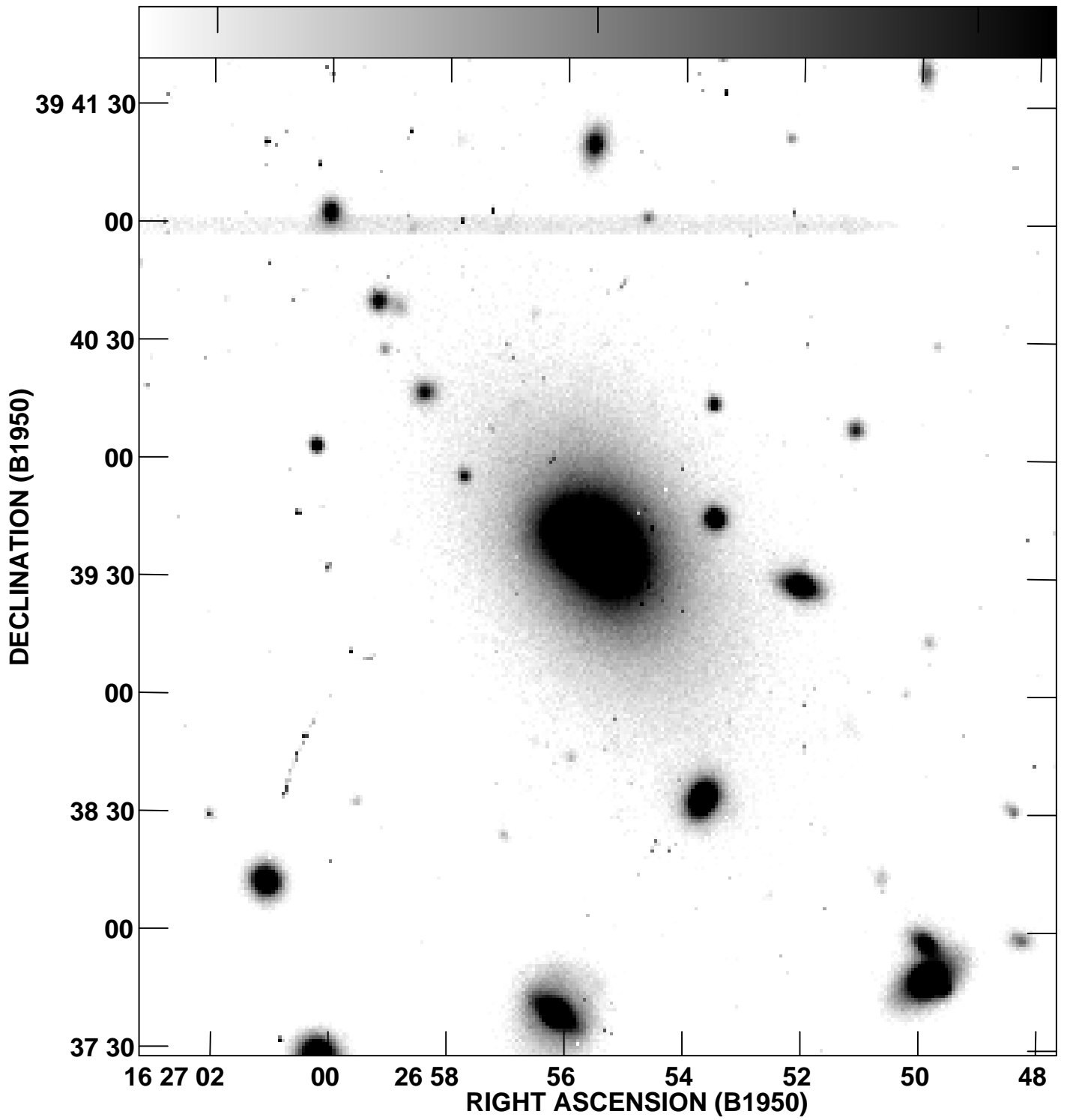
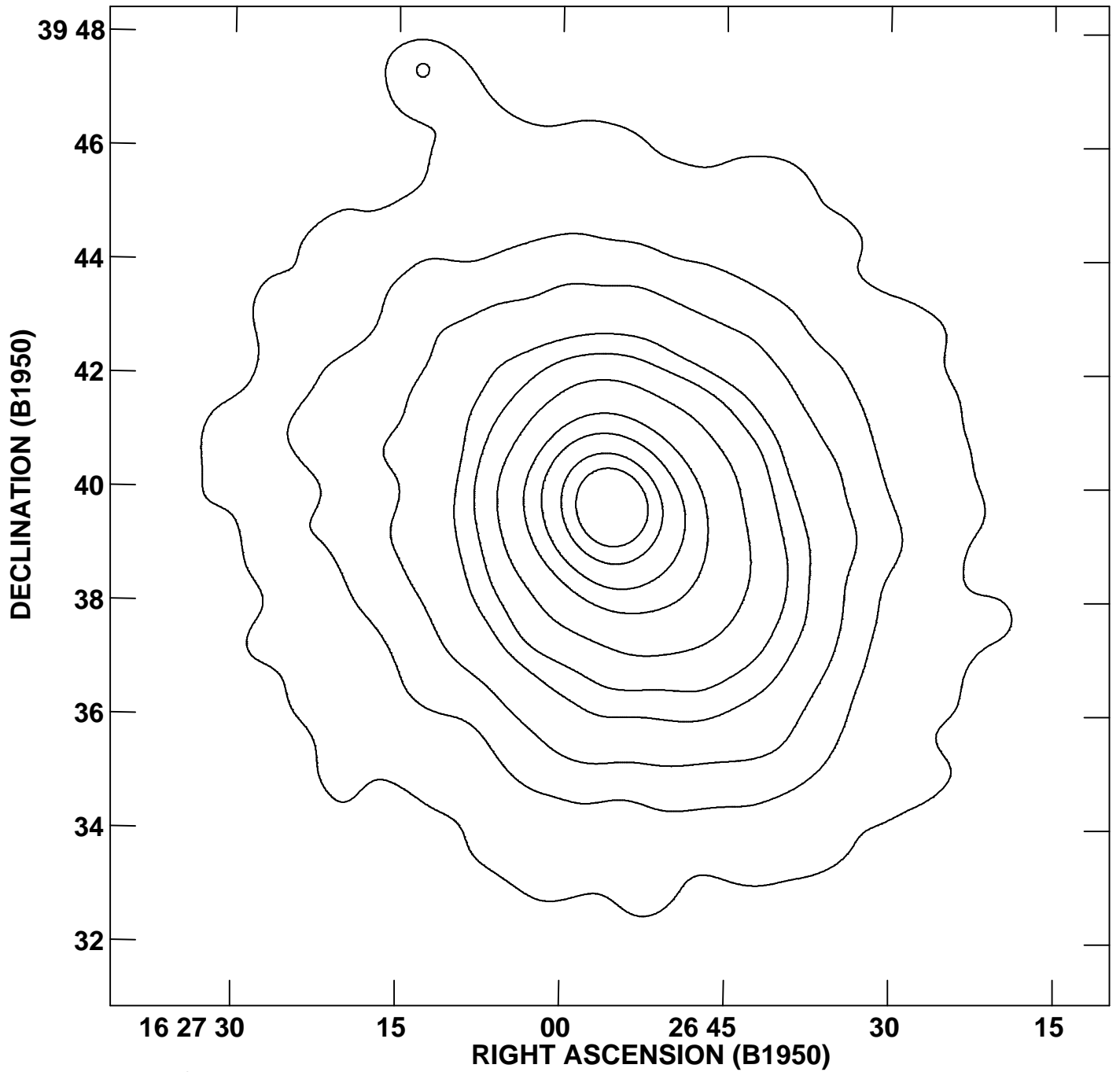


Figure 9: Radio/X-ray overlay





Peak flux = 7.2593E+03
Levs = 7.2593E+02 * (0.500, 0.700, 0.900,
1.250, 1.500, 2.000, 3.000, 4.000, 5.500,
7.000)

